Second

PROGRESS REPORT
(Project SR-109)

on

EFFECT OF GRAIN SIZE AND CARBON CONTENT ON THE LOW TEMPERATURE TENSILE PROPERTIES OF HIGH PURITY Fe-C ALLOYS

by

R. L. SMITH, G. SPANGLER AND R. M. BRICK
University of Pennsylvania

Transmitted through

**NATIONAL RESEARCH COUNCIL'S
COMMITTEE ON SHIP STEEL**

Advisory to

SHIP STRUCTURE COMMITTEE

MAY 28, 1954

SHIP STRUCTURE COMMITTEE

MEMBER AGENCIES:

BUREAU OF SHIPS, DEPT. OF NAVY

MILITARY SEA TRANSPORTATION SERVICE, DEPT. OF NAVY

UNITED STATES COAST GUARD, TREASURY DEPT.

MARITIME ADMINISTRATION, DEPT. OF COMMERCE

AMERICAN BUREAU OF SHIPPING

ADDRESS CORRESPONDENCE TO:

SECRETARY

SHIP STRUCTURE COMMITTEE

U. S. COAST GUARD HEADQUARTERS

WASHINGTON 25, D. C.

May 28, 1954

Dear Sir:

As part of its research program related to the improvement of hull structures of ships, the Ship Structure Committee is sponsoring an investigation of the mechanical properties of binary alloys of iron at low temperatures at the University of Pennsylvania. A paper covering portions of this work was presented before the midwinter meeting of the American Society of Metals, March 4 and 5, 1954. This report entitled "Effect of Grain Size and Carbon Content on the Low Temperature Tensile Properties of High Purity Fe-C Alloys" by R. L. Smith, G. Spangler and R. M. Brick is being distributed by the Committee as SSC-81, the Second Progress Report on this project.

The project is being conducted with the advisory assistance of the Committee on Ship Steel of the National Academy of Sciences-National Research Council.

Any questions, comments, criticism or other matters pertaining to the Report should be addressed to the Secretary, Ship Structure Committee.

This Report is being distributed to those individuals and agencies associated with and interested in the work of the Ship Structure Committee.

Yours sincerely,
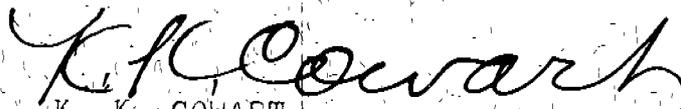
K. K. COWART
Rear Admiral, U. S. Coast Guard
Chairman, Ship Structure
Committee.

EFFECT OF GRAIN SIZE AND CARBON CONTENT ON THE LOW TEMPERATURE TENSILE PROPERTIES OF HIGH PURITY Fe-C ALLOYS

By R. L. Smith, G. Spangler and R. M. Brick

Abstract

Several low carbon ferrites, approximately 99.9+% pure apart from added carbon and substantially free of oxygen, nitrogen and hydrogen, were prepared and tested in tension under various conditions of heat treatment, ferrite grain size, and test temperature. True stress-strain curves were calculated and the significant tensile parameters evaluated.

Ferrite grain size was shown to be the sole factor determining ductility of 0.02% carbon alloys at liquid air temperature; decreasing the grain size causes a remarkable increase in ductility. With more than 0.02% carbon, carbide morphology has an important effect on the ductility. Heat treatments which resulted in carbides at the grain boundaries materially reduced the low temperature ductility.

The exponent of strain hardening was found to decrease with decreasing temperature, increasing carbon content, and increasing grain size. The initial presence of a substructure or a decrease in grain size markedly increased the yield stress at liquid air temperatures. Twinning was not found to contribute to the low temperature brittleness.

N UMEROUS investigations on the low temperature behavior of ferritic steels have been conducted in the last decade. Because of the interaction of variables such as impurity elements, distribution of second phase, grain size and mechanical variables, the results obtained from such investigations cannot be interpreted in fundamental terms. For example it is known that a decrease in

grain size lowers the transition temperature from ductile to brittle behavior. However, the methods used to vary grain size have been such that the beneficial effects could also be attributed solely to some less obvious cause.

It has long been known that fine-grained ferrites retain their tensile ductility to a lower temperature than coarse-grained ferrites (1, 2)[1]. Several investigators have determined the effect of ferrite grain size on the impact strength of various low carbon steels (3, 4, 5, 6, 7). In a few cases, no significant variation in transition temperature was reported. Generally, however, impact transition temperature has been found to increase with increasing grain size, changing as much as 30 °F with an increase in grain size of one ASTM number. These investigations were conducted on commercial ferrites. In most cases, the different grain sizes were obtained by significantly different heat treatments. In some instances, thin sheet stock or wires were tested where size effect complicated the test results. However, all of these investigations have shown that the effect of grain size must be determined quantitatively if the mechanical properties are to be evaluated unambiguously.

In contrast to this, N. P. Allen (8) has reported that variation of the grain size by subcritical anneals does not affect the impact transition temperature or general properties of "pure" irons tested at the National Physical Laboratory, whereas different grain sizes obtained by supercritical heat treatments and varying cooling rates altered the properties considerably.

This paper is the result of an investigation designed to delineate the effect of carbon content and ferritic grain size on the mechanical properties of relatively pure ferrites as determined by the axial tension test over a range from room temperature to liquid air temperature.

ALLOY PREPARATION

Some alloys were prepared by melting a high-grade electrolytic iron under strongly oxidizing conditions and slagging with lime. Carbon was added by dropping sugar charcoal directly on the surface of the oxidized melt. These air-melted alloys were remelted in high-fired beryllia crucibles in a high frequency vacuum melting furnace. The initial FeO:C reaction was controlled by conducting the actual melting under nearly an atmosphere of evolved gases and then slowly evacuating to a pressure of less than one micron.

A second approach was to melt electrolytic iron under strongly oxidizing conditions and cast the metal, high in FeO, into a slab which was first hot-rolled and then cold-rolled to a thickness of about 0.010 inch. This thin stock was deoxidized in dried (−190 °C dew point) hydrogen at 1100 °C (2010 °F) for 6 weeks. The hydrogen-

---

[1]The figures appearing in parentheses pertain to the references appended to this paper.

deoxidized stock was then remelted in vacuo in a high-fired BeO crucible with a sufficient amount of high purity carbon to produce the desired carbon content. No significant difference in either chemical analysis (Table I) or mechanical properties has been observed between alloys made by the two different methods of preparation.

Table I
Analyses of Iron-Carbon Alloys

	Hydrogen-Deoxidized Iron-Carbon Alloy	Carbon-Deoxidized Iron-Carbon Alloy
C	0.02	0.03
Mn (Spectrographic)	0.0005	0.0005
Mn (Wet Method)	0.003	0.002
Si	0.005	0.001
Be	0.0013	0.0007
Ni	0.0008	<0.0003
Cr	0.0004	0.0004
O (NBS)*	0.0006	0.0007
(BMI)†	0.0010	0.0014
N (NBS)*	0.0008	0.0011
(BMI)†	0.0003	0.0004
H (NBS)*	nil	0.00007
(BMI)†	<0.00004	<0.00004

*Average of duplicate vacuum fusion analyses by National Bureau of Standards, courtesy J. G. Thompson.
†Duplicate vacuum fusion analyses by Battelle Memorial Institute, courtesy C. E. Sims.
NOTE: The amount of each element present, other than carbon, is near the limit of experimental error of the available analytical methods. Therefore, although two to four times as much nitrogen or oxygen, for example, is reported by one laboratory as compared to another, the differences generally are not significant, since the amount present is in the vicinity of 0.000X%.

The alloy ingots were hot-forged to 1-inch rounds, hot-rolled to ⅝-inch square bars, then air-cooled and cleaned. These bars were vacuum-annealed at 1000 °C (1830 °F) for 100 hours to eliminate gas absorbed during hot working. The annealed stock was cold-rolled and heat treated in vacuum or helium to the desired grain size. The heat treated bars were then machined to tensile specimens having a 1-inch gage length by 0.200-inch diameter. The bars were given a final hand polish with 600 emery paper.

Mechanical Testing at Low Temperatures

The mechanical testing of the tensile specimen was done in a hydraulic testing machine provided with special equipment for low temperature work (9, 10, 11).

The specimen was submerged in a suitable refrigerant kept at the desired constant low temperature. The cooling fluid was contained in a Dewar vessel, supported around the test bar without interfering with the movements of the specimen grips and their alignment. Such a setup is shown schematically in Fig. 1. By use of a flexible bellows, alignment of the grips during the test takes place freely without being hindered by the rather weighty test vessel. Practically ideal self-alignment during the test was obtained by use of case-hardened chains to transfer the tensile force to the specimen.

The cooling media used in this investigation were liquid air for —185 °C and Freon No. 12, cooled by liquid air, for the range —150 to 30 °C. Temperatures were regulated by an automatic control circuit. An air bubbler stirring arrangement was used to keep the temperature as uniform as possible.

Natural stress-strain data were obtained at low temperatures using a microformer-type diameter gage immersed with the test speci-
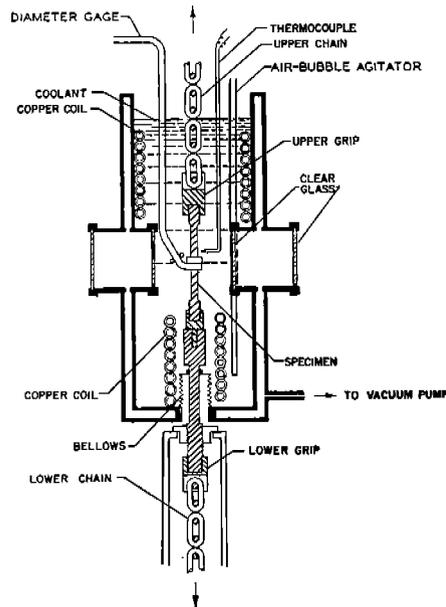
Fig. 1—Schematic Diagram of Tensile-Test Apparatus.

men in the heat transfer fluid (Fig. 2). A strain pacer was connected in series with the diameter gage and an autographic recorder. The investigator traverses the gage length of the specimen with the jaws of the diameter gage. While the specimen is decreasing in diameter, the diameter gage causes the strain pacer pointer to rotate clockwise. If the spacing of the jaws of the diameter gage increases by leaving the neck, the pacer reverses its direction of rotation. Thus it is readily possible to find the region of necking and then to remain in the position of minimum diameter.

EFFECT OF TEMPERATURE, CARBON AND FERRITIC GRAIN SIZE ON TOTAL STRAIN

In order to evaluate the effect of grain size on tensile ductility, most of the tests for this investigation were conducted at liquid air

temperature. At this temperature, the differences in total strain appear to be most marked (Fig. 10). The test is rapid and economical of material. At liquid air temperature, the total strain is usually relatively small and reasonably reproducible. Post-fracture measurements on the fractured specimens agree within 0.002 of an inch with
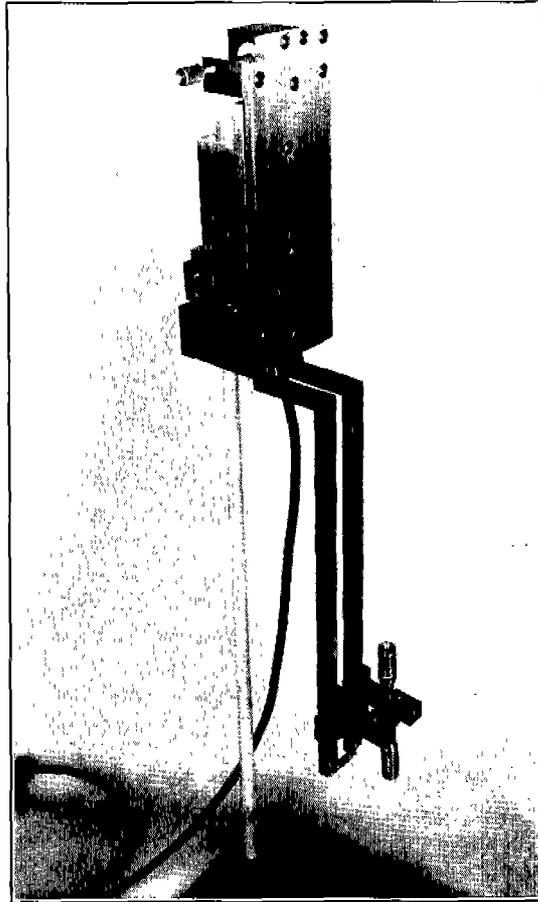
Fig. 2—Recording Diameter Gage Used in Tensile Testing.

the diameter gage measurements at the neck of the specimen recorded at the instant of fracture. On the other hand, for the low carbon alloys at room temperature, ellipticity and a rim effect on the order of 0.010 inch may obscure the strain measurements.

A plot of ferrite grain size versus total strain at liquid air temperature for an 0.02% carbon alloy, Fig. 3, shows a nearly linear relation of marked slope. A grain size change of one ASTM number
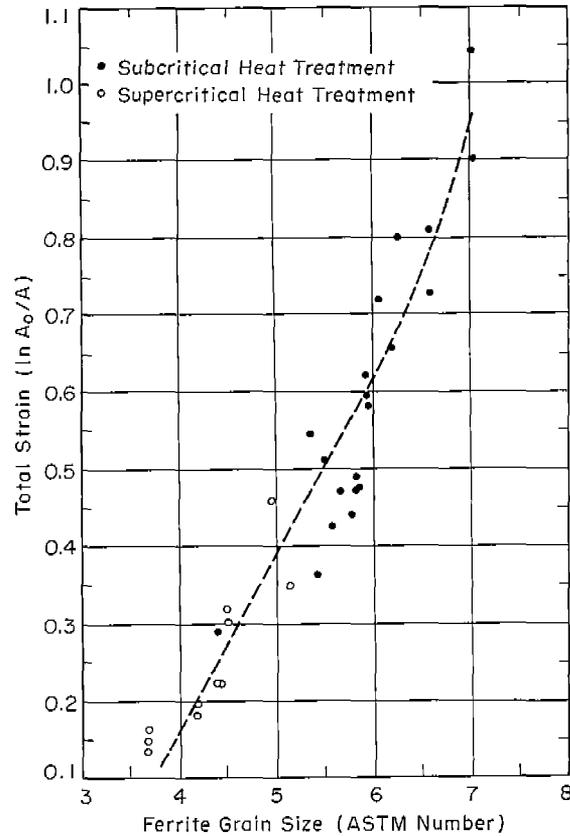
Fig. 3—Effect of Ferrite Grain Size on Total Strain
at Liquid Air Temperature. (0.02% carbon alloy.)

changes the total strain by about 0.2. The grain size was varied by heat treatment at different temperatures, by use of varied times, or by varying the amount of cold work prior to heat treatment. Details of the heat treatments used are given in Table II. When the same grain size was obtained by heating at different temperatures, the same total strain at liquid air temperature was obtained. This is good evidence to support the rather remarkable conclusion that for this 0.02% carbon alloy, the ductility at liquid air temperature is solely determined by grain size.

Further examination of the data in Table II shows that in most cases the larger grain sizes were obtained by means of a heat treatment above the A_1 temperature, Fig. 5. If solution and precipitation of Fe_3C from ferrite were significant, then cooling at different rates from the maximum solubility temperature (723 °C) should also result in differences in ductility, due to retained solution of carbon or its

Table II

Tensile Data for Iron - 0.02% Carbon Alloy

Spec. No.	Temp. °C	Grains per in² at ×100	Total Strain	Upper Yield	Lower Yield	Flow Stress at 0.15 Strain	Flow Stress at 0.20 Strain	Uniform Strain	Exponent of Strain Hardening n	Heat Treatment °C
10	+23	...	2.028	31.8	26.9	44.7	49.0	0.382	0.326	620, A.C. 1 hr.
9	+23	...	2.150	30.8	27.6	44.8	49.5	0.390	0.340	620, A.C. 1 hr.
5	−29	...	2.350	37.2	34.1	49.0	53.0	0.332	0.296	620, A.C. 1 hr.
13	−29	22	2.397	43.4	34.3	48.5	53.0	0.366	0.317	620, A.C. 1 hr.
3	−84	...		57.4	49.1	Tem. Control Lost After Lower Yield				620, A.C. 1 hr.
2	−89	...	2.170	57.5	50.8	62.0	65.5	0.192	0.174	620, A.C. 1 hr.
8	−152		1.410	85.4	77.5	94.0	99.5	0.178	0.191	620, A.C. 1 hr.
1	−153		1.470	84.7	77.8	94.0	99.0	0.185	0.186	620, A.C. 1 hr.
T	−185	64	1.062	99.3	100.2	119.4	127.6	0.241	0.234	500, A.C. 18 hr.
U	−185	67	0.904	99.6	99.6	Str. Rt. Control Lost			0.220	500, A.C. 18 hr.
28B	−185	43	0.810	96.7	98.1	118.9	126.0	0.228	0.208	620, A.C. 10 hr.
27B	−185	39	0.800	97.9	95.7	117.0	123.0	0.202	0.198	620, A.C. 1 hr.
27A	−185	49	0.727	95.4	98.2	118.9	125.9	0.274	0.206	620, A.C. 10 hr.
28A	−185	34	0.722	91.8	95.1	117.0	124.5	0.218	0.201	710, A.C. 1 hr.
35B	−185	37	0.656	92.8	91.1	116.4	123.3	0.238	0.190	620, F.C. 1 hr.
40	−185	30	0.624	92.8	92.7	117.5	124.9	0.241	0.214	620, A.C. 20 min.
42	−185	31	0.595	91.2	94.3	117.6	125.0	0.226	0.210	620, F.C. 4 hr.
41	−185	31	0.582	94.8	92.1	116.7	123.0	0.226	0.202	620, F.C. 4 hr.
7	−185	21	0.544	89.2	92.1	116.5	123.0	0.177	0.192	620, A.C. 1 hr.
H	−185	23	0.512	92.4	89.2	116.2	123.0	0.176	0.198	723, A.C. 3 hr.
11	−185	22	0.492	95.7	93.4	117.5	124.0	0.185	0.184	620, A.C. 1 hr.
45	−185	29	0.475	97.7	97.8	118.9	126.5	0.253	0.196	620, A.C. 1 hr.
46	−185	29	0.474	93.3	99.2	118.6	126.2	0.229	0.192	723, Q. 1.5 hr.
G	−185	26	0.470	85.5	94.5	117.0	123.2	0.180	0.196	850, A.C. ¾ hr.
L	−185	15	0.457	89.7	86.4	113.9	120.1	0.214	0.194	723, F.C. ¾ hr.
D	−185	28	0.440	91.6	91.4	116.8	123.0	0.178	0.196	723, A.C. 15 min.
E	−185	24	0.425	94.1	89.7	117.6	124.7	0.195	0.200	620, A.C. 20 min.
4	−185	22	0.361	100.3	93.7	119.0	125.0	0.181	0.181	930, Q. 20 min.
Q	−185	18	0.346	95.5	104.9	122.2	128.7	0.213	0.178	930, A.C. 20 min.
N	−185	12	0.317	97.8	98.0	120.8	127.5	0.205	0.184	930, A.C. 1 hr.
O	−185	12	0.300	86.3	100.0	123.9	130.0	0.201	0.166	700, A.C. ½ hr.
W	−185	11	0.293	90.4	none	118.8	124.1	0.158	0.165	895, A.C. ½ hr.
M	−185	11	0.226	89.0	none	117.8	124.5	0.181	0.190	895, A.C. 20 min.
L	−185	11	0.226	104.1	none	118.0	123.6	0.157	0.162	930, Q. 20 min.
S	−185	9	0.195	96.6	106.5	126.0	.....	0.168	0.168	930, Q. 20 min.
P	−185	9	0.180	90.8	98.8	123.0	.....	0.180	0.176	750, A.C. 10 min.
K	−185	6	0.159		none	122.6	.....		0.164	930, F.C. 10 min.
43	−185	6	0.146	91.7	none	.....	.....	et	0.194	930, A.C. 10 min. 750, F.C.
44	−185	6	0.133	93.3	none	.....	.....	et	0.188	930, F.C. 10 min. 750, A.C.

precipitation with different cooling rates. It can be seen that specimens quenched, air-cooled, and furnace-cooled from this temperature and tested within a week do not vary significantly in total strain at −185 °C. Apparently, then, quench aging is not a factor affecting ductility of unnotched tensile specimens of this pure 0.02% carbon alloy. It is shown later that heat treatment affects the yield stress values considerably.

Fig. 6 shows the grain size versus total strain values at liquid air temperature for an alloy of 0.04% carbon. At this carbon level, stringers of carbides oriented parallel to the rolling direction were present in all specimens that were cold-rolled and recrystallized below the A_1 temperature, Fig. 7. A few scattered areas of free pearlite
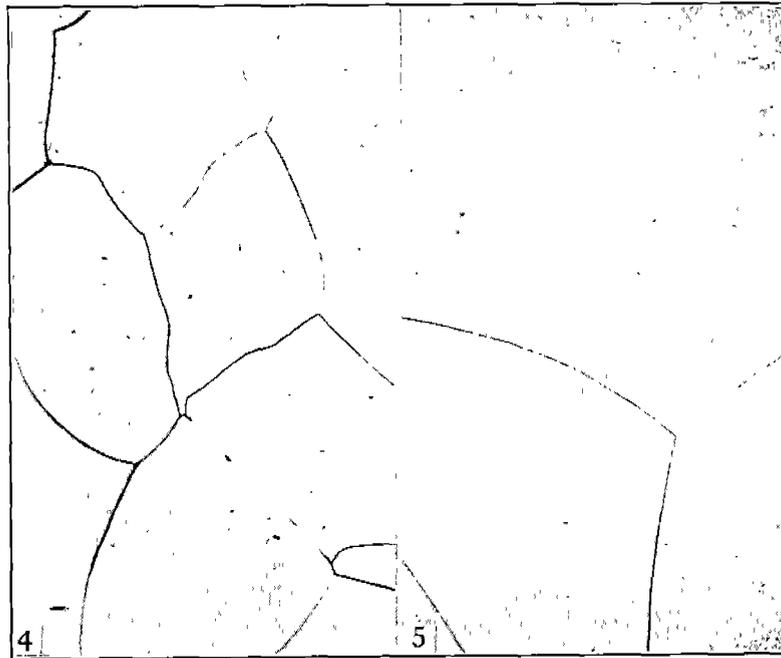
Fig. 4—0.02% Carbon Alloy Heat Treated 1 Hour 620 °C, Air-Cooled. Nital etch. × 750.

Fig. 5—0.02% Carbon Alloy Heat Treated 20 Minutes 930 °C, Furnace-Cooled to 750 °C, Air-Cooled. Nital etch. × 750.

and networks of discontinuous grain boundary carbides were visible in this 0.04% carbon alloy when heat treated above the A_1 temperature, Fig. 8. The various heat treatments for this alloy are given in Table III.

The points representing the subcritical heat treatments show a grain size effect on liquid air ductility nearly the same as the lower carbon alloy (0.02% carbon) represented by the dashed line. The points representing the supercritical heat treatments of this alloy lie well below the scatter band of the 0.02% carbon alloy. Therefore, for this alloy, heating above the A_1 gives less ductility than heating below the A_t. This can be seen by examining the values for an ASTM number 5 where the spread is from $\varepsilon = 0.546$ (42% R.A.) for a subcritical recrystallization to $\varepsilon = 0.063$ (6% R.A.) for a supercritical recrystallization. This difference shows that with carbon present in excess of the solubility limit, carbide morphology as well as grain size controls low temperature ductility. Carbides in the 0.04% carbon supercritically heated alloy were generally at ferrite grain boundaries or grain junctions.

Reheating the supercritically recrystallized specimens at 600 °C for 4 hours improved the ductility by about 0.1 natural strain or 20%.
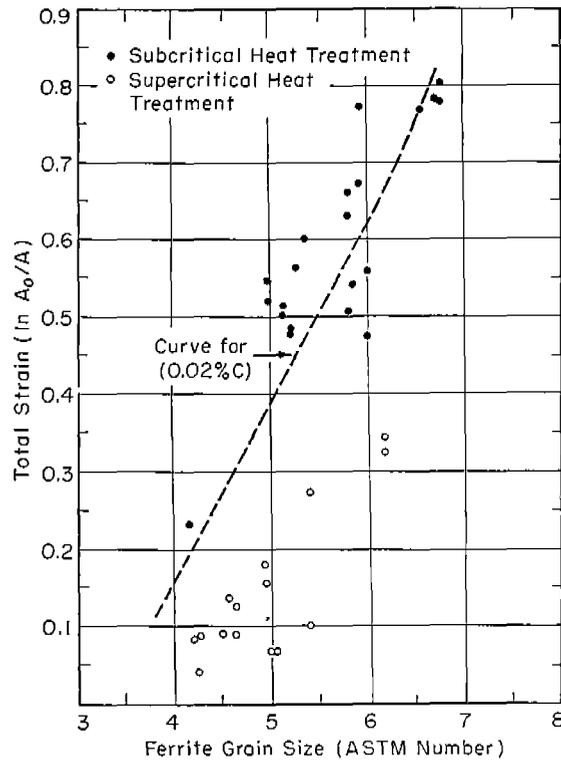
Fig. 6—Effect of Ferrite Grain Size on Total Strain at Liquid Air Temperature. (0.04% carbon alloy.)

Perhaps longer times of tempering might increase this value materially. On the other hand, it may be that unless the specimens are recrystallized subcritically, no time of tempering would be sufficient to overcome the embrittling effect of carbides at ferrite grain boundaries. Attempts at spheroidization by cycling through the A_1 temperature resulted in abnormal grain growth.

Fig. 9 shows the total strain at liquid air temperature versus grain size for two higher carbon alloys (0.05 and 0.12% carbon), co-plotted with data for the 0.02% carbon alloy (Table IV). It can be seen that although the grain size varies considerably, the total strain for these two alloys as subcritically heat treated remains essentially constant. At these higher carbon contents, two opposing variables are affecting the ductility; i.e., with increasing time of isothermal subcritical heat treatment, the ferrite grain size increases and the carbides tend to spheroidize. The two opposing factors appear to balance each other for these higher carbon alloys so that the net change in ductility is not significant.
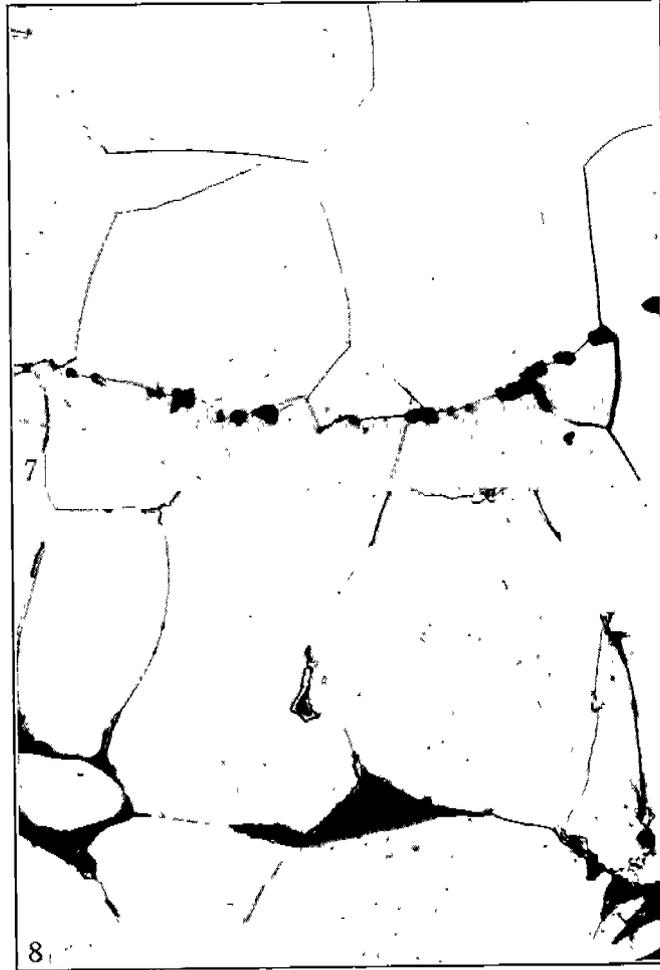
Fig. 7—0.04% Carbon Alloy Heat Treated 1 Hour 650 °C, Air-Cooled. Nital etch. × 750.
Fig. 8—0.04% Carbon Alloy Heat Treated 10 Minutes 920 °C, Furnace-Cooled to 840 °C, Air-Cooled. Nital etch. × 750.

For a given grain size and heat treatment, it can be seen that the 0.05% carbon alloy is always more ductile; i.e., shows greater total strain than the 0.12% carbon alloy. However, the limiting heat treatment at 600 °C (1110 °F) for 96 hours which spheroidizes the carbides, making them relatively ineffective, results in a total strain for both of these higher carbon alloys equal to that of the low, 0.02% carbon alloy of the same grain size. This is evidence that ferrite grain size has the same effect on total strain for the higher carbon alloys that it does for the lower carbon alloys, provided it can be separated

Table III
Tensile Data for Iron - 0.04% Carbon Alloy

Spec. No.	Temp. °C	Total Strain	Grain/inch² at X 100	Heat Treatment °C
28	+26	1.394	15	10 min. 920, F.C. / 840, A.C.
29	+26	1.345	15	10 min. 920, F.C. / 840, A.C.
30	+26	1.570	58	1 hr. 650, A.C.
31	+26	1.500	58	1 hr. 650, A.C.
52	−105	1.560	47	1 hr. 650, A.C.
53	−102	1.479	45	1 hr. 650, A.C.
55	−100	1.361	13	10 min. 920, F.C. / 840, A.C.
54	−100	1.275	15	10 min. 920, F.C. / 840, A.C.
26	−185	0.805	54	26 hrs. 600, A.C.
27	−185	0.780	54	26 hrs. 600, A.C.
E	−185	0.779	52	1 hr. 650, A.C.
63	−185	0.774	31	45 min. 700, F.C.
D	−185	0.769	49	1 hr 650, A.C.
64	−185	0.673	31	45 min. 700, F.C.
24	−185	0.665	28	26 hrs. 600, A.C.
24X	−185	0.632	28	26 hrs. 600, A.C.
9	−185	0.604	21	4.5 hrs. 600, A.C.
11	−185	0.565	20	48 hrs. 600, A.C.
41	−185	0.558	32	45 min. 700, Q.
12	−185	0.546	16	94 hrs. 600, A.C.
46	−185	0.543	29	45 min. 700, A.C.
13	−185	0.520	16	94 hrs. 600, A.C.
7	−185	0.514	18	26 hrs. 600, A.C.
44	−185	0.505	32	45 min. 700, A.C.
6	−185	0.502	18	26 hrs. 600, A.C.
8	−185	0.486	19	4.5 hrs. 600, A.C.
10	−185	0.478	19	48 hrs. 600, A.C.
40	−185	0.475	32	45 min. 700, Q.
16	−185	0.345	37	10 min. 920, A.C.
17	−185	0.326	37	10 min. 920, A.C.
45	−185	0.274	22	30 min. 800, A.C.
5	−185	0.231	9	26 hrs. 600, A.C.
32	−185	0.181	16	10 min. 920, F.C. / 840, A.C. / temp. 4.5 hrs. 600, A.C.
33	−185	0.156	16	10 min. 920, F.C. / 840, A.C. / temp. 4.5 hrs. 600, A.C.
15	−185	0.126	13	10 min. 920, F.C. / 840, A.C.
14	−185	0.133	12	45 min. 700, A.C.
47	−185	0.100	22	30 min. 800, A.C.
1	−185	0.090	13	10 min. 920, F.C. / 840, A.C.
4	−185	0.090	11	45 min. 700, A.C.
2	−185	0.084	9	45 min. 700, A.C.
39	−185	0.063	16	10 min. 920, F.C. / 840, A.C.
38	−185	0.063	16	10 min. 920, F.C. / 840, A.C.
3	−185	0.039	10	10 min. 920, F.C. / 840, A.C.

from the carbide morphology. This does not necessarily hold true for grain sizes attained other than by recrystallizing below the A_1 temperature.

In attempting further to separate the effect of carbon content on ductility from that of grain size, a series of tests were run at three temperatures: room temperature, −100 °C, and liquid air temperature (Fig. 10). The results show that the difference in ductility resulting from these two specific heat treatments is three to four times as great at liquid air temperature as at room temperature. This diver-

Fig. 9—Effect of Ferrite Grain Size on Total Strain at Liquid Air Temperature.

Table IV
Tensile Tests at Liquid Air Temperature

0.05% Carbon Alloy

Specimen No.	Total Strain	Grain Size grain/inch at × 100	Heat Treatment °C
31a	0.756	89	1 hr. 600, A.C.
31b	0.761	88	1 hr. 600, A.C.
34a	0.835	69	10 hrs. 600, A.C.
34b	0 704	58	10 hrs. 600, A.C.
33a	0.705	43	96 hrs. 600, A.C.
33b	0.820	43	96 hrs. 600, A.C.
11	0.049	15	10 min. 910, F.C.
			820, A.C.
7	0 054		10 min. 910, F.C.
			820, A.C.

0.12% Carbon Alloy

33a	0.534	82	1 hr. 600, A.C.
33b	0.544		1 hr. 600, A.C.
33c	0.652		10 hrs. 600, A.C.
33d	0.680	63	10 hrs. 600, A.C.
33e	0.632	30	96 hrs. 600, A.C.
33f	0 644		96 hrs. 600, A.C.
31	0.070	21	10 min. 900, F.C.
			780, A.C.
27	0.094		10 min. 900, F.C.
			780, A.C.

gence at liquid air temperature is due to the major effect of grain size on ductility at liquid air temperature and it is this effect which masks the effect of carbon content on ductility.

In summation, it appears that the major factor determining the ductility at liquid air temperature of high purity iron containing 0.02% carbon is ferrite grain size. For the 0.02% carbon alloy, there

is no effect of heat treatment or cooling rate other than its effect on grain size. For the higher carbon, 0.03 to 0.12% carbon alloys, there is in addition the effect of heat treatment on the state of the carbides. Supercritical heat treatments, which result in carbides or pearlite at ferrite grain boundaries, materially reduce low temperature ductility. Subcritical annealing of cold-worked structures, which gives spheroidized carbides aligned in the testing direction, considerably or completely eliminates their detrimental effect.
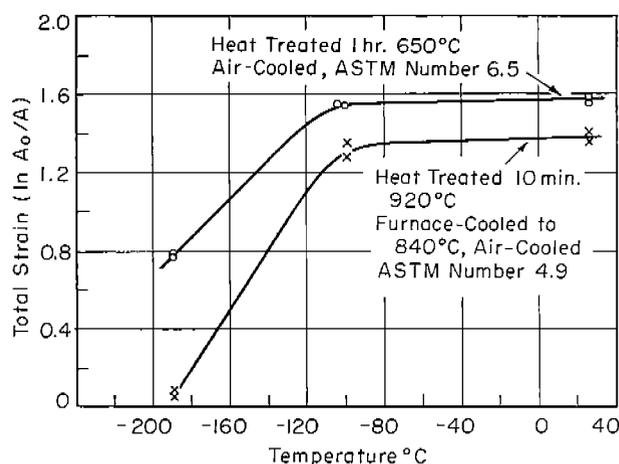
Fig. 10—Effect of Temperature on Total Strain. (0.04% carbon alloy.)

The above observations apply with certainty only to high purity alloys containing substantially no oxygen or nitrogen.

EFFECT OF CARBON AND FERRITE GRAIN SIZE ON STRAIN HARDENING

Although the slope of the plastic region of the stress-strain curve is frequently used to evaluate strain hardening, it is not a satisfactory indicator in the case of the low carbon ferrites reported here. This is illustrated by Fig. 11 showing the uniform strain regions of two tensile specimens tested at two different temperatures. It is apparent that temperature affects the upper yield, lower yields, and yield point elongation. An examination of points (a) and (b) at a given constant strain reveals that, for the example shown here, the instantaneous rate of strain hardening, $d\sigma/d\varepsilon$, is greater at the low temperature. However, such a comparison does not have any fundamental significance because of the difference in strain history prior to strain, $\varepsilon = 0.12$. A comparison of $d\sigma/d\varepsilon$ values at constant strains from the minimum in the stress-strain diagrams is somewhat more meaningful, as it is a measure of the ability of the material to strain harden after
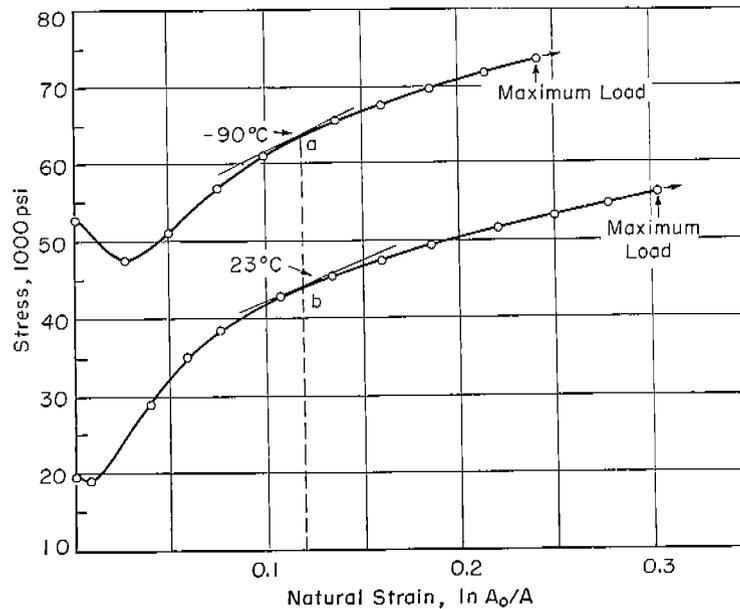
Fig. 11—Natural Stress-Strain Curves for Iron-Carbon Alloy Containing 0.03% Carbon.

the start of uniform deformation (12). Even this comparison is somewhat nebulous, as it has been shown that the inherent ability of a material to work harden is affected by the deformation history (13).

It is common to talk of $d\sigma/d\varepsilon$ in the linear region of the true stress-strain curve. Since $d\sigma/d\varepsilon$ remains constant in this range, the limitation of comparing it at some constant strain is removed. For ferrites and, in fact, for most materials this linearity begins at the point of maximum load and continues in the early stages of necking (Fig. 12). However, the triaxial stresses imposed by the formation of a neck require that a correction be made by subtracting the transverse stress components, thus reducing the slope of this portion of the stress-strain diagram (14). The amount of this correction depends upon the severity of the neck. If the shape of the neck were the same under all conditions of testing, it would be possible to utilize relative changes in $d\sigma/d\varepsilon$. There is no reason to assume that this would be the case. On the contrary, there is evidence that the opposite is true.

Necking is a manifestation of localization of deformation. If conditions are such as to accentuate this localization, e.g., lowering the temperature, it seems that the radius of the neck would decrease. It has been shown that increasing the speed of testing increases the
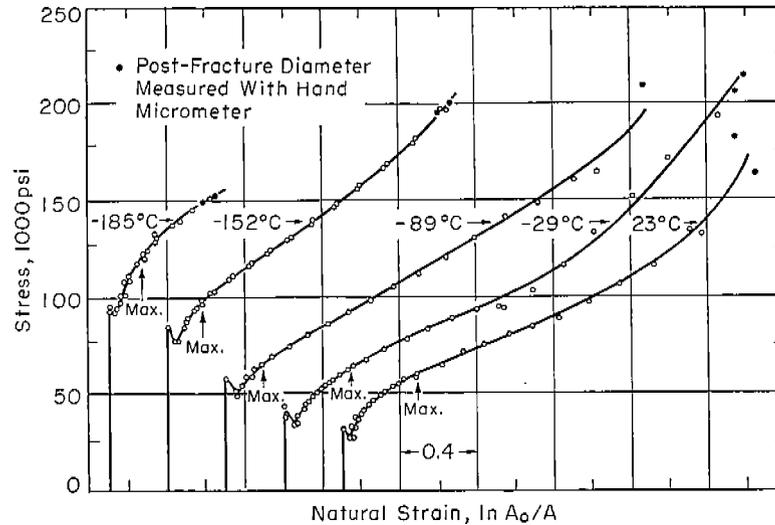
Fig. 12—Natural Stress-Strain Curves for Iron-Carbon Alloy Containing 0.02% Carbon.

severity of necking (15). In ferrites, increasing the strain rate has been found to be comparable to decreasing the temperature. This implies that a greater correction for triaxiality would be necessary at the lower temperature of testing. This correction might easily be large enough so that the slope of the linear portion of the stress-strain curve would show a decrease with a decrease in the temperature of testing. Unless a valid correction is applied for triaxiality, $d\sigma/d\varepsilon$ cannot be used as a measure of strain hardening over the linear portion of the stress-strain curve.

A commonly used measure of strain hardening is that designated as the strain hardening exponent (n) in the well-known equation $\sigma = K\varepsilon^n$. This is the rate of change of the logarithm of true stress with respect to the logarithm of natural strain, $d\ln\sigma/d\ln\varepsilon$, and can be shown to be numerically equal to the strain at maximum load (16, 17, 18). Experimentally, the relationship $\sigma = K\varepsilon^n$ is reasonably valid in the uniform strain region or between the lower yield point and maximum load. This is illustrated by a typical curve as shown in Fig. 13.

Necking strain is not as important as uniform strain in governing the absorption of energy, since this requires a relatively large volume of deformed metal. Gensamer (19) has shown the importance of the plastic properties in determining energy absorption by their ability to control the distribution, or localization, of strain. He pointed out that the strain gradient, $d\varepsilon/dx$, may depend, not on the capacity for deformation as measured by reduction of area or other principal
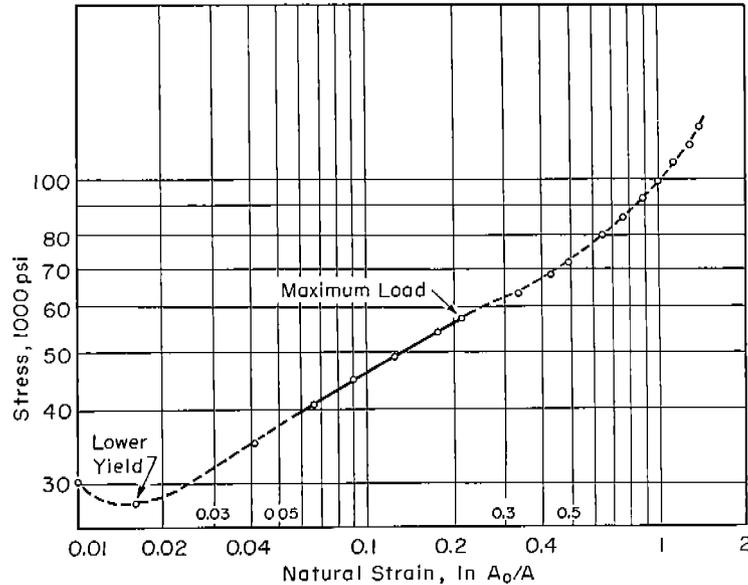
Fig. 13—Typical Plot of Log Stress Versus Log Strain.

strains at fracture, but on strain hardening as measured by the strain hardening exponent. By differentiation of the expression $\sigma = K\varepsilon^n$ he found the strain gradient to be inversely proportional to the exponent of strain hardening, i.e., $d\varepsilon/dx \propto 1/n$. A brittle material would be one where strain is localized, resulting in a small amount of uniform strain, a high strain gradient and correspondingly a low strain hardening exponent.

Although the relation $\sigma = K\varepsilon^n$ is of limited application, it is useful in that n is as good a measure of strain hardening as can be obtained for materials exhibiting heterogeneous yielding; therefore this paper reports the variation of the strain hardening exponent with temperature, grain size, and carbon content.

It was pointed out above that $n = \varepsilon_\mu$, where $\varepsilon_\mu =$ strain at maximum load. For this investigation, although the strain values for maximum load are reported in nearly all cases, the numerical values are subject to some uncertainty. Maximum load holds over a considerable range of strain. Uniform strain was taken at the drop in load at the end of this range, but this drop occurs very slowly and was difficult to observe accurately. Nonlinearity often occurs before the drop in load at the maximum. For these reasons, uniform strain is not as reproducible a measure of the exponent of strain hardening as the slope, $d \ln \sigma / d \ln \varepsilon$.

It should be emphasized at this point that n and $d\sigma/d\varepsilon$ are not
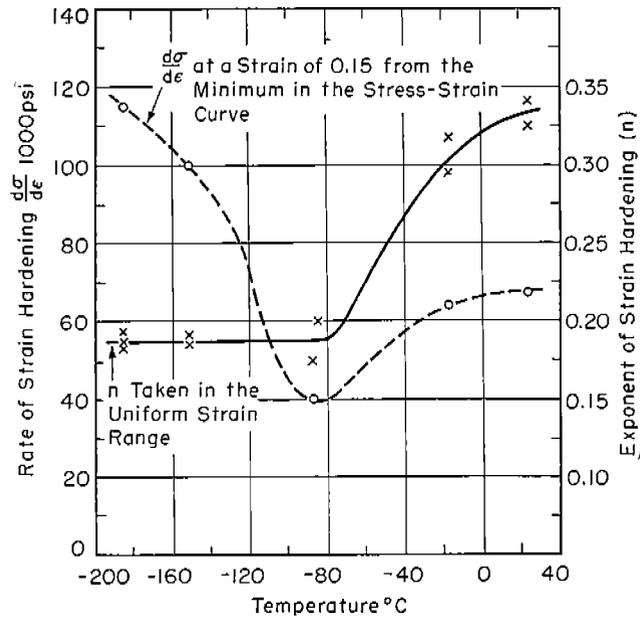
Fig. 14—Effect of Temperature on Strain Hardening. (0.02% carbon alloy heat treated subcritically.)

equivalent, even in an approximate sense. G. V. Smith (20) pointed out that it is often erroneously assumed that n and $d\sigma/d\varepsilon$ vary in a like manner. Fig. 14 is presented showing n versus temperature for the 0.02% carbon alloy co-plotted with $d\sigma/d\varepsilon$ versus temperature taken at a constant strain of $\varepsilon = 0.15$ from the minimum in the stress-strain curve. Whereas (n) decreases from room temperature to —100 °C and then remains constant to liquid air temperature, $d\sigma/d\varepsilon$ decreases from room temperature to —90 °C, and then rises sharply from —90 °C to liquid air temperature! The instantaneous rate of strain hardening, $d\sigma/d\varepsilon$, for this alloy obtained from the expression $d\sigma/d\varepsilon = n(\sigma/\varepsilon)$ also agrees with the value of $d\sigma/d\varepsilon$ obtained graphically. This should serve to emphasize the necessity of differentiating between the apparent rate of strain hardening, $d\sigma/d\varepsilon$, and the exponent of strain hardening, n.

Hollomon (21) found that increasing the carbon content or decreasing the temperature increased the slope of the linear portion of the stress-strain curve. This observation has been confirmed by others and forms the basis for the often-repeated statement that "strain hardening" increases with decreasing temperature. It is important to keep in mind that this applies to necking strain and that a correction for triaxiality could reverse this trend.

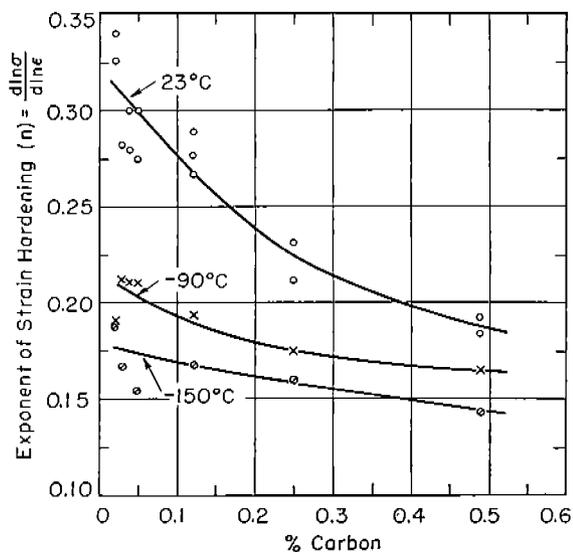The strain hardening exponent need not change in a like manner.

Fig. 15—The Effect of Carbon on the Exponent of Strain Hardening. All heat treatments are supercritical except for the 0.02% carbon alloy.
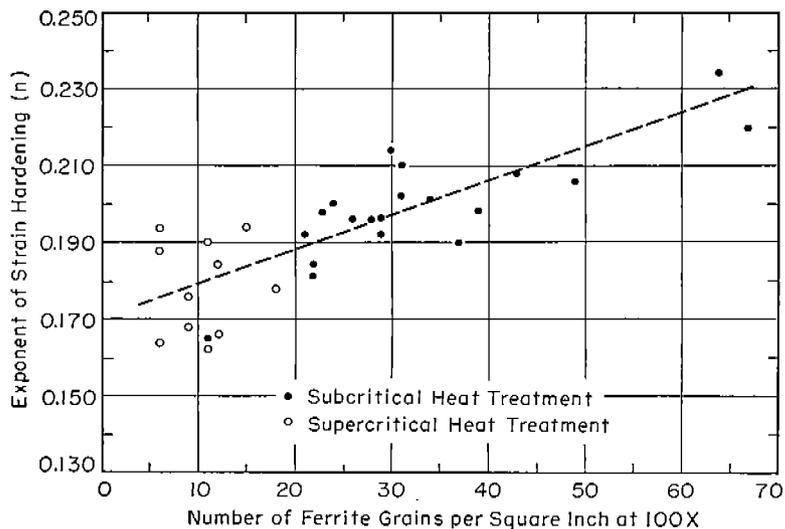

Fig. 16—Effect of Ferrite Grain Size on the Strain Hardening Exponent of an 0.02% Carbon Alloy Tested at Liquid Air Temperature.

This is illustrated in Fig. 15, which shows the exponent of strain hardening decreasing with increasing carbon content and decreasing temperature. A decrease in the grain size is seen to increase the

exponent of strain hardening (n) at liquid air temperature (Fig. 16).

The observed decrease of n with increasing grain size and with decreasing temperature would increase the strain gradient and tend to restrict deformation to a relatively small volume. This restriction correlates satisfactorily with the embrittlement effects of low temperature and large grain size.

Thus it appears that although $d\sigma/d\varepsilon$ and n are mathematically related, they do not behave similarly in relation to other variables such as temperature, carbon content and grain size. The expression $\sigma = K\varepsilon^n$ holds during the period of uniform strain for ferrites. The exponent of strain hardening, n, is found to decrease, generally, with decrease of temperature, increase of carbon content, and increase of grain size. It is this measure of strain hardening that directly affects the distribution of deformation in a given material. Additional support for this perhaps tenuous evidence that strain hardening of ferrite is less at low temperatures and that this is important with regard to low temperature brittleness is offered by the fact that, for copper, the strain hardening exponent n increases with decrease in temperature (29).

EFFECT OF FERRITE GRAIN SIZE AND TEMPERATURE ON THE YIELD POINT

It is well known that decreasing the size of the ferrite grains of mild steel increases the flow stresses at room temperature (22, 23). Data illustrating the grain size effect on yield points at liquid air temperature for the 0.02% alloy are shown in Fig. 17. Here upper yield stress is plotted as a function of grain size. Lower yield stress behaves in the same manner.

The curve drawn through solid points, representing subcritically heat treated specimens, shows the expected grain size effect. However, the open-circle points representing supercritically heat treated specimens show a still greater effect on the yield point for an essentially constant grain size! A careful examination in Table II of yield stresses for duplicate test specimens will show that the scatter in this plot is not due to poor alignment of specimens, surface imperfections or inadequate fillets, since in most cases duplicate test specimens have nearly the same yield stress.

Such a plot as this should clearly emphasize the danger of extending to other temperatures generalizations that are valid at one temperature. In this case it is believed that it is safe to say that, at liquid air temperature, decreasing the grain size increases the yield stress. However, unlike its effect on total strain, grain size is clearly not the major variable governing yield stress.

An examination of the microstructure of supercritically heat treated specimens (Fig. 5) revealed the presence of a veined sub-

structure which was absent in the subcritically heat treated specimens. Higher heat treatment temperatures and faster cooling rates generally gave higher yield points and in these specimens veining was more readily detected. The conditions for veining in ferrites have been discussed at length by Hultgren and Herrlander (24). The substructures observed in the supercritically heat treated specimens presumably were caused by the volume change in the $\gamma \rightleftarrows \alpha$ transfor-
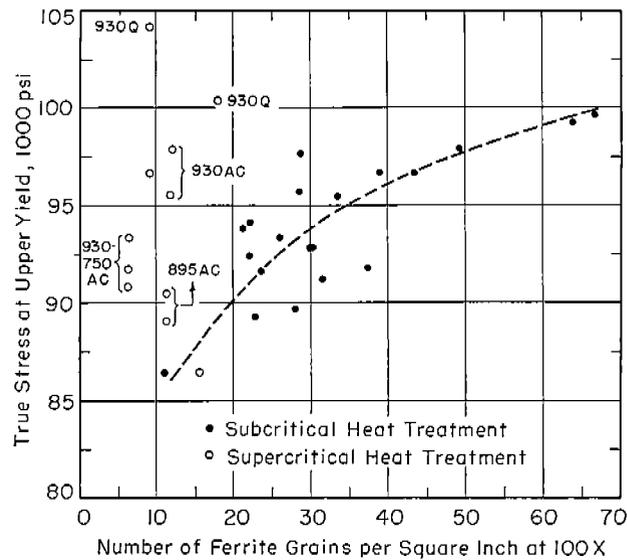

Fig. 17—Effect of Ferrite Grain Size on the Upper Yield Point at Liquid Air Temperature. (0.02% carbon alloy.)

mation. This volume change induces stresses in some grains sufficient to deform them slightly. Subcritically recrystallized and unstrained grains did not show veining substructures.

Cottrell's theory is universally known and generally accepted as being the most logical explanation of the yield point phenomenon (25). If this theory is extended to include the effects of substructures, observations of this investigation, e.g., Fig. 17, are rather simply explicable.

Cottrell utilizes the concept that solute atoms (interstitial carbon and nitrogen in iron) diffuse to, and lock, dislocations. A stress that is sufficient to tear the dislocations loose from their solute atmospheres is greater than that necessary to keep them moving; thus the load drops at the initial yield. A grain boundary can be regarded as an array of dislocations, and when the boundary contains solute atoms, distributed so that the strain energy is reduced, yielding cannot easily start from or propagate through grain boundaries. Upon

application of stress, a number, (n), of dislocations move within the grain from regions of high stress concentration until they are stopped by the grain boundary. These dislocations produce a force against the grain boundary which is (n) times the force exerted by one dislocation. These dislocations add to the externally applied stress and force dislocations out of the grain boundaries. The larger the grain, the greater the number of dislocations piled up at the grain boundary; thus a lower applied stress is required to initiate yielding. The theory does not require that grain boundaries be present for yielding, since the criterion here is the initiation of yielding within the grain.

With the above concept in mind, consider two test specimens identical in all respects except that one possesses a substructure as a result of a particular heat treatment. The substructure boundaries would affect yield stresses qualitatively the same as primary grain boundaries, by interfering with dislocations moving through the lattice. Since decreasing the grain size increases the yield stress, it is probable that the presence of such a substructure would tend to nullify the effect of larger grains. Although subgrain boundaries act to impede the motion of dislocations, it is likely that the dislocations move more easily from such boundaries than from regular grain boundaries.

In evaluating the possible effect of initial substructure on fracture, it should be kept in mind that, for iron, slip may take place on many planes containing the $<111>$ close-packed direction, whereas cleavage or brittle fracture is almost wholly restricted to the cube planes. The disregistry of subgrains is small so that fracture does not have to change direction appreciably in propagating along a cube plane. In contrast, the difference in orientations between neighboring grains is large, thus requiring a large change in direction of fracture. Decreasing the grain size increases the number of changes of path of transcrystalline fracture appreciably, whereas the creation of a substructure causes a relatively small increase in changes of fracture path.

It is to be expected that impurity atoms will have a tendency to segregate at grain boundaries and, in the case of oxygen atoms, initiate cleavage there (30). Not only are clusters of impurity atoms sites of relatively high stress concentration but in most cases they form sites which do not slip easily. Small grains offer a greater total surface area over which to distribute impurity atoms than do large grains. This reduces the concentration per unit area and minimizes the probability of formation of clusters of a brittle phase large enough to form microcracks. It is likely that at some given applied stress, fracture initiates in a region of high stress concentration where the yield point is high in comparison to the surrounding material and then propagates through the grain along cleavage planes. Intergranular fracture is not likely (except in the presence of a large amount of an embrittling impurity such as oxygen), since the fracture

path would require a considerable change in direction. The above mechanism could be the reason why there is such a marked increase in total strain at $-185\ °C$ with a decrease in grain size. Likewise, the observed pronounced effect of grain size on low temperature ductility supports the concept of impurity segregation at grain boundaries.

The presence of mechanical twins in ferrite has been well established. For the strain rates used in this investigation (approximately $10^{-4}\ sec^{-1}$), twinning occurred below about $-100\ °C$. It should be noted that for specimens which have an appreciable ductility at liquid air temperature, extensive twinning is present. An examination of the curves in Figs. 14 and 16 reveals that the exponent of strain hardening, n, decreases with increasing grain size and decreasing temperature; but that (n) remains essentially constant at temperatures below that where twinning is encountered for the specified strain rate. We might conclude from this that the formation of twins acts in the same manner as grain boundaries in that twinning increases (n), thus counteracting the tendency of temperature to decrease (n). On the basis of this analysis, it may be postulated that the presence of twin boundaries, if anything, acts to increase ductility.

The effect of temperature on yielding has been thoroughly discussed by Cottrell and Bilby (26). The extension of temperature effects to the plastic region is limited to a qualitative explanation and is not readily amenable to a mathematical analysis. However, it does not appear logical that temperature effects should cease to be of importance after the completion of yielding.

A temperature dependence probably occurs through thermal fluctuations of the dislocation loops. Seitz states, "If dislocations can tie each other down as indicated by Frank, then thermal fluctuations at the point of locking can be important in breaking the dislocations loose" (27). In this mechanism, it is assumed that the applied stress causes the bowing out between obstacles and the thermal fluctuations simply act in joining the sides of the bows. The amount of blocking of dislocations is dependent on temperature, and thermal fluctuations seem to be necessary to aid the movement of dislocations if they are to be moved with the addition of small applied stress. In the absence of thermal fluctuations of sufficient magnitude, the applied stress must be higher to remove the blocking. At some point, the stress necessary to move anchored dislocations may be so large that fracture along a cleavage plane is the preferred process.

Mott (28) points out that the most effective agents for locking impurities are to be expected in lattices other than face-centered cubic. For a solute atom to interact with a screw dislocation, it may be necessary for it to strain the lattice unequally in different directions. Cottrell (25) points out that this is probably because the field around a screw dislocation is primarily shear stress with practically no hydro-

static component. Solute atoms which distort the lattice equally in all directions can interact with a hydrostatic stress field, but, in order to interact with a shear stress, the distortion must not be spherically symmetrical. The tetragonal distortion that carbon and nitrogen produce in iron leads to a nonspherical distortion, but according to Cottrell there are no known principles which would lead one to expect nonspherical distortions around solute atoms in a face-centered cubic lattice. Thus solute atoms would be expected to anchor only edge dislocations in face-centered cubic metals, but both edge and screw dislocations are anchored by interstitial atoms in body-centered cubic metals. A row of interstitial carbon atoms in iron exerts a strong interaction extending only over a short distance, a situation that is favorable for the introduction of pronounced thermal effects such as the decrease in total strain with decrease in temperature that is observed in ferrites.

CONCLUSIONS

1. The sole factor determining the ductility under uniaxial tension at liquid air temperature of high purity iron containing 0.02% carbon is ferrite grain size. For the 0.02% carbon alloy, there is no effect of heat treatment or cooling rate other than its effect on grain size.

2. In the case of higher carbon, 0.03 to 0.12% carbon alloys, liquid air ductility is determined by grain size and by the state of the carbides. Supercritical heat treatments which result in carbides or pearlite at ferrite grain boundaries or junctions materially reduce low temperature ductility. Subcritical annealing of cold-worked structures which gives aligned spheroidized carbides may considerably or completely eliminate their detrimental effect, at least on ductility in the rolling direction.

3. The exponent of strain hardening, n, decreases with decreasing temperature, increasing carbon content and increasing grain size. This strain hardening exponent appears to be more significant, with respect to low temperature ductility, than the slope of the uncorrected natural stress-strain diagram.

4. The initial presence of a substructure or a decrease in grain size markedly increases the yield stress at liquid air temperatures.

5. The total strain under uniaxial tension decreases rapidly with decreases in temperature below about -100 °C (the exact temperature depends upon grain size). It is probable that the following three factors contribute to this low temperature embrittlement:

    (a) The loss of thermal aid in moving dislocations.

    (b) The effectiveness of interstitial solute atoms in a body-centered cubic lattice in blocking dislocations.

    (c) The effect of a decreased value of the strain hardening

exponent 'n' in restricting the distribution of deformation.

6. There seems to be no reason to postulate that twinning is a significant contributing factor to low temperature brittleness.

References

1. Z. Jeffries, "Effect of Temperature, Deformation and Grain Size on the Mechanical Properties of Metals", *Transactions,* American Institute of Mining and Metallurgical Engineers, Vol. 60, 1919, p. 474.

2. L. Seigle, M.S. Thesis, University of Pennsylvania, 1948.

3. J. B. Austin, "Manufacture of Steels for Low-Temperature Service", United States Department of Commerce, National Bureau of Standards, Circular 520, May 1952, p. 36.

4. S. J. Rosenberg and D. H. Gagon, "Effect of Grain Size and Heat Treatment Upon Impact Toughness at Low Temperatures of Medium Carbon Forging Steel", TRANSACTIONS, American Society for Metals, Vol. 30, 1942, p. 361.

5. J. Gorrissen, "Some Notes on Brittleness in Mild Steel", *Journal,* Iron and Steel Institute, Vol. 162, 1949, p. 16.

6. J. M. Hodge, R. D. Manning and H. M. Reichhold, "The Effect of Grain Size on Notch Toughness", *Journal of Metals,* Vol. 1, 1949, p. 233.

7. H. W. Gillett and F. T. McGuire, "Behavior of Ferritic Steels at Low Temperatures", National Research Council, War Metallurgy Committee Report No. W-78, June 1944.

8. N. P. Allen, "Recent European Work on the Mechanical Properties of Metals at Low Temperatures". Symposium on the Mechanical Properties of Metals at Low Temperatures, 1952, published by United States Department of Commerce, National Bureau of Standards, Circular 520.

9. H. T. Green, Ph.D. Dissertation, University of Pennsylvania, June 1952.

10. R. P. Steijn and R. M. Brick, "Flow and Fracture of Single Crystals of High Purity Ferrite", TRANSACTIONS, American Society for Metals, Vol. 46, 1954.

11. R. L. Smith, R. V. Fostini and R. M. Brick. "The Low Temperature Properties of Relatively High Purity Iron-Carbon Alloys", First Progress Report, Ship Structure Committee, Project SR-109, Serial No. SSC52, August 1952.

12. G. W. Geil and N. L. Carwile, "Tensile Properties of Copper, Nickel, and Some Copper-Nickel Alloys at Low Temperatures", Symposium on the Mechanical Properties of Metals at Low Temperatures, 1952, Published by United States Department of Commerce, National Bureau of Standards, Circular 520.

13. J. E. Dorn, A. Goldberg and R. E. Tietz, "The Effect of Thermal-Mechanical History on the Strain Hardening of Metals", *Metals Technology,* Vol. 15, September 1948.

14. P. W. Bridgman, "The Stress Distribution at the Neck of a Tension Specimen", TRANSACTIONS, American Society for Metals, Vol. 32, 1944, p. 533.

15. A. Nadai, "Theory of Flow and Fracture of Solids", 1950, McGraw-Hill Book Company, New York City.

16. J. H. Hollomon, "Tensile Deformation", *Transactions,* American Institute of Mining and Metallurgical Engineers, Vol. 102, 1945, p. 162.

17. M. Gensamer, "The Yield Point in Metals", *Transactions,* American Institute of Mining and Metallurgical Engineers, Vol. 128, 1938, p. 104.

18. E. Voce, "The Relationship Between Stress and Strain for Homogeneous Deformation", *Journal,* Institute of Metals, Vol. 74, 1948, p. 537.

19. M. Gensamer, "Strength and Ductility", TRANSACTIONS, American Society for Metals, Vol. 36, 1946, p. 30.

20. G. V. Smith, "Strain Hardening—Effects of Alloying Elements and Micro-structure", Symposium on the Cold Working of Metals, October 1948, published by the American Society for Metals.

21. J. H. Hollomon, "The Effect of Heat Treatment and Carbon Content on the Work Hardening Characteristics of Several Steels", TRANSACTIONS, American Society for Metals, Vol. 32, 1944, p. 123.

22. C. A. Edwards and L. B. Pfeil, "The Tensile Properties of Single Crystals and the Influence of Crystal Size Upon the Tensile Properties of Iron", *Journal,* Iron and Steel Institute, Vol. 112, 1925, p. 79.

23. J. Winlock and R. Leiter, "Some Factors Affecting the Plastic Deformation of Sheet and Strip Steel and Their Relation to the Deep Drawing Properties", TRANSACTIONS, American Society for Metals, Vol. 25, 1937, p. 163.

24. Hultgren and Herrlander, "Hot Deformation Structures, Veining and Red Shortness Cracks in Iron and Steel", *Transactions,* American Institute of Mining and Metallurgical Engineers, Vol. 172, 1947, p. 493.

25. A. H. Cottrell, "The Yield Point in Single Crystal and Polycrystalline Metals", Symposium on the Plastic Deformation of Crystalline Solids, May 1950, Joint Sponsorship of Carnegie Institute of Technology and the Department of the Navy Office of Naval Research.

26. A. H. Cottrell and B. A. Bilby, "Dislocation Theory of Yielding and Strain Aging of Iron", *Proceedings,* Physical Society, Vol. 62A, 1949, p. 49.

27. F. Seitz, "The Theory of Plastic Flow in Single Crystals", Symposium on the Plastic Deformation of Crystalline Solids, May 1950, Joint Sponsorship of Carnegie Institute of Technology and the Department of the Navy Office of Naval Research.

28. N. F. Mott, "Mechanical Strength and Creep in Metals", Symposium on Imperfections in Nearly Perfect Crystals, October 1950, John Wiley and Sons, Inc., New York City.

29. R. M. Brick, "Behavior of Metals at Low Temperatures", published by American Society for Metals, 1953, p. 1.

30. F. L. Vogel and R. M. Brick, "Deformation of Ferrite Single Crystals", American Institute of Mining and Metallurgical Engineers, *Journal of Metals,* Vol. 4, No. 5, May 1953, p. 700.